We are IntechOpen,
the world's leading publisher of
Open Access books
Built by scientists, for scientists

6,900
Open access books available

186,000
International authors and editors

200M
Downloads

Our authors are among the

154
Countries delivered to

TOP 1%
most cited scientists

12.2%
Contributors from top 500 universities

Interested in publishing with us?
Contact book.department@intechopen.com

Numbers displayed above are based on latest data collected.
For more information visit www.intechopen.com

Control and Identification of Chaotic Systems by Altering the Oscillation Energy

Valery Tereshko
University of the West of Scotland
United Kingdom

1. Introduction

Last years, researchers paid a major attention to the controlling chaos schemes that use information obtained from the experimental time series of system's accessible variables. When the trajectory is in a neighbourhood of desired UPO, the Ott-Grebogi-Yorke (OGY) controlling chaos scheme can be applied (Ott et al., 1990). Exploiting the linearity of return map near corresponding unstable fixed point, it stabilizes UPOs with one unstable direction by directing the trajectory to the orbit stable manifold. The technique requires performing several calculations to generate a control signal. This approach may fail (i) if the dynamics is so fast that the controller cannot follow it, and (ii) if the dynamics is highly unstable, i.e. the trajectory diverges from a target so far that small perturbations cannot be effective. For highly dissipative systems that are well characterized by a one-dimensional return map, occasional proportional feedback (Hunt, 1991; Peng et al., 1991) and occasional feedback (Myneni et al., 1999) techniques was developed. The occasional proportional feedback utilizes an amplitude of parametric perturbation that is proportional to the deviation of system's current state from its desired state (Hunt, 1991; Peng et al., 1991). Similar technique but with application to a system accessible variable instead of a parameter is called proportional perturbation feedback (Garfinkel et al., 1992). Alternatively, occasional feedback utilizes a control pulse duration that is equal to the transit time of trajectory through a specified window placed on either side of saddle fixed point (Myneni et al., 1999). Owing to simplicity, these methods do not require any processor and can be implemented at high speeds.

For highly unstable orbits, quasicontinuous extensions of original OGY technique can be applied when more than one control points per period are taken (Hübinger et al., 1994; Reyl et al., 1993). Another option is to use a continuous-time control (Gauthier et al., 1994; Just et al., 1999b; Pyragas, 1992; 1995; Socolar et al., 1994). However, obtaining complete information about desired trajectory can be difficult (or even impossible, say, at high frequencies or spatial complexity). Therefore, the continuous-time delayed feedback using information only about a period of desired UPO became most popular. Here, the control signal is proportional to the difference between a system current state and its state at some earlier time, the delay being set to a period of desired UPO (Gauthier et al., 1994; Pyragas, 1992). This approach is found effective to control low-period UPOs at high frequencies (Gauthier et al., 1994), but it may fail for high-period UPOs or for highly unstable orbits (Just et al., 1999b). An extension of method that incorporates information from many previous states of the system is suitable for controlling UPOs in fast dynamical systems, with large value of Lyapunov exponents, and of

high periods (Socolar et al., 1994). The attractiveness of delayed feedback scheme consists in the self-organizing ability of a system to autosynchronize its own behaviour. However, unlike the OGY-based schemes where the trajectory is targeted to a predefined UPO, the delayed feedback control does not discriminate between different periodic orbits of the same period, and does not necessarily lead to the stabilization of orbits embedded in a chaotic attractor (Hikihara et al., 1997; Simmendinger et al., 1998). The success of this control is significantly restricted by a control loop latency (Just et al., 1999a).

In the nonfeedback, or open-loop, schemes, the control signal does not depend on a system state. One of approaches is a nonlinear entrainment method (Hübler & Lüscher, 1989; Jackson & Hübler, 1990). It requires knowledge of the system equations to construct control forces that can have large amplitude and complicated shape. The basins of entrainment, in turn, can have very complicated structure. Typically, this method can require as many control forces, as there are dimensions of the system.

In contrast, there are many examples of converting chaos to a periodic motion by exposing a system to only one, weak periodic force or weak parameter modulation (Alexeev & Loskutov, 1987; Braiman & Goldhirsch, 1991; Cao, 2005; Chacón, 1996; Chacón & Díaz Bejarano, 1993; Chizhevsky & Corbalán, 1996; Chizhevsky et al., 1997; Dangoisse et al., 1997; Fronzoni et al., 1991; Kivshar et al., 1994; Lima & Pettini, 1990; Liu & Leite, 1994; Meucci et al., 1994; Qu et al., 1995; Ramesh & Narayanan, 1999; Rödelsperger et al., 1995; Tereshko & Shchekinova, 1998). Typically, this approach utilizes only a period and an amplitude of perturbation (Alexeev & Loskutov, 1987; Braiman & Goldhirsch, 1991; Kivshar et al., 1994; Lima & Pettini, 1990; Liu & Leite, 1994; Ramesh & Narayanan, 1999). If the amplitude is kept small enough, one can expect a controlled periodic orbit or an equilibrium to trace closely the corresponding unperturbed one (provided that no crises are induced). The periodic perturbation methods can be easily realized in practice. However, the independence of the perturbation from a system state leads to some limitations of above approach: the control by periodic perturbations relying only on their period and amplitude is not, in general, a goal-oriented technique (Shinbrot et al., 1993). On the other hand, the importance of a phase (Cao, 2005; Chacón, 1996; Chizhevsky & Corbalán, 1996; Chizhevsky et al., 1997; Dangoisse et al., 1997; Fronzoni et al., 1991; Meucci et al., 1994; Qu et al., 1995; Tereshko & Shchekinova, 1998) and even a shape (Azevedo & Rezende, 1991; Chacón, 1996; Chacón & Díaz Bejarano, 1993; Rödelsperger et al., 1995) of perturbation became evident. The utilization of extra parameters allows tuning the perturbation to a desired target shape more selectively. The above findings were generalized in a concept of geometrical resonance that reveals the underlying mechanism of nonfeedback resonant control for a general class of chaotic oscillators (Chacón, 1996). The phase of perturbation is crucial for the success of nonfeedback resonant control. First of all, it determines the direction and, hence, the targets where a trajectory is driven to. Secondly, keeping the perturbation precisely in phase with the controlled signal ensures smallest control amplitudes, whereas dephasing can destroy the control. By changing only the perturbation phase, one can switch the trajectory from one controlled state to another (Tereshko & Shchekinova, 1998).

In real-life systems, the existing uncontrolled drifts can spoil resonant conditions. Small deviation of the perturbation frequency from the resonance is equivalent to slowly varying modulation of the phase. This results in a temporal evolution consisting of regular alternations between a stabilized orbit and the chaotic behaviours (Chizhevsky & Corbalán, 1996; Meucci et al., 1994; Qu et al., 1995). The real-life nonfeedback control may, thus, demand an occasional

adjustment of the perturbation frequency. To overcome the above problem, a feedback control where the perturbation depends on the controlled signal can be used.

Have analyzed the existing approaches, we developed a following control method. To any type of system behaviour, we put in correspondence a value of averaged oscillation energy that is an averaged (over the time) compound of the system kinetic and potential energy. The objective is to alter this energy so as to correspond to a desired behaviour. This is a general approach that does not depend on particular oscillator equations. Simple feedback depending solely on an output signal is utilized for this purpose. We start with identifying the type of control perturbations appropriate for the above control. One simply increases the feedback strength, and, thus, depending on the perturbation phase, increases or decreases the oscillation energy. The above strategy does not require any computation of the control signal and, hence, is applicable for control as well as identification of unknown systems. The above approach was applied to control isolated oscillators, as well as coupled ones (Tereshko, 2009; Tereshko et al., 2004a;b). Here, we summarize the obtained results and present our new findings in controlling spatially-extended systems.

2. General approach

Let us consider controlling a general type nonlinear oscillator

$$\ddot{x} + \chi(x,\dot{x}) + \xi(x) = F(t) + g(x,\dot{x}) \tag{1}$$

where $\chi(x,\dot{x})$, $\xi(x)$ and $g(x,\dot{x})$ are dissipative or energy-generating component, restoring force, and control force, respectively. These functions are nonlinear in general case. Also, $\chi(x,\dot{x})$ and $g(x)$ are assumed not to contain an additive function of x. $F(t)$ is an external time-dependent driving force.

At $F(t) = 0$ and $g(x,\dot{x}) = 0$, Eq. (1) possesses the equilibriums defined by equation $\xi(x) = 0$. In oscillators with nonlinear damping (say, van der Pol and Reyleigh oscillators), an equilibrium becomes unstable at some parameter values, and stable self-sustained oscillations are excited. In other types of oscillators, say Duffing oscillator, a limit cycle arises under the action of periodic driving force. We assume that at some driving amplitudes, a limit cycle becomes saddle, and new attractor, say period-2 cycle, arises. In many well-known examples, this scenario leads, through the sequence of bifurcations, to the birth of chaotic attractor.

One can define an energy of oscillations as the sum of "potential" and "kinetic" energy:

$$E(t) = \int \xi(x)\,\mathrm{d}x + \frac{1}{2}\dot{x}^2 . \tag{2}$$

An averaged (over period T) energy yields

$$\langle E \rangle = \frac{1}{T}\int_0^T \left(\int \xi(x)\,\mathrm{d}x + \frac{1}{2}\dot{x}^2 \right)\mathrm{d}t . \tag{3}$$

For periodic dynamics T is an oscillation period, whereas for chaotic one $T \to \infty$. Each attractor of an oscillator is assigned to a value of averaged energy (3). If an oscillation amplitude is sufficiently small, the limit cycle oscillations can be approximated as $x \simeq \rho \sin \omega t$, which gives $\langle E \rangle = \frac{1}{2}\rho^2$.

Typically, transitions to a chaotic attractor correspond to the increase of energy (3). Let us clarify this statement on the example of a period-doubling process. Suppose that changing some of the system parameters results in an oscillation period doubling and, eventually, in a

chaos. Starting at period-1 cycle, its amplitude grows with increasing the above parameter, and, hence, energy (3) does. Every period-doubling bifurcation contributes subharmonic (as well as its odd harmonic) to the fundamental frequency, which again increases energy (3). Thus, the higher the orbit period is, the higher the averaged energy corresponding to this orbit. A stationary point, around which a limit cycle develops, can be viewed as a zero-amplitude cycle possessing, thus, zero energy.

A following control strategy can be proposed. Starting at a lower energy attractor, one stabilizes higher energy repellors by sequential increasing the averaged oscillation energy. On the contrary, decreasing this energy leads to the stabilization of lower energy repellors. A change of energy (2) yields

$$\dot{E}(t) = \xi(x)\dot{x} + \dot{x}\ddot{x} = \left(-\chi(x,\dot{x}) + F(t) + g(x,\dot{x})\right)\dot{x}. \tag{4}$$

The last term of (4) represents an energy change caused solely by the control. We require that

$$g(x,\dot{x})\,\dot{x} > 0\ (< 0) \tag{5}$$

for $\forall(x,\dot{x})$. A minimal feedback satisfying (5) is achieved at $g = g(\dot{x})$. Indeed, simple linear (relative to the velocity) control $g(\dot{x}) \sim \dot{x}$ as well as nonlinear controls of higher power, say $g(\dot{x}) \sim \dot{x}^3$ suffice. In general

$$g(\dot{x}) = k\,h(\dot{x}) \tag{6}$$

where $h(\dot{x})$ is assumed to be odd, i.e. $h(\dot{x}) = -h(-\dot{x})$. One can, thus, define

$$h(\dot{x}) \begin{cases} > 0, & \text{if } \dot{x} > 0 \\ = 0, & \text{if } \dot{x} = 0 \\ < 0, & \text{if } \dot{x} < 0. \end{cases} \tag{7}$$

To guarantee a control perturbation tininess even at high values of $\dot{x}$, $h(\dot{x})$ is taken to be bounded. Throughout, we consider $g(\dot{x}) = k\tanh(\beta\dot{x})$ with $0 < \beta \leqslant \infty$ determining the function slope.

Perturbation (6-7) is specially tuned to control equilibriums: their positions are not changed by the control as the latter vanishes at $\dot{x} = 0$. $\dot{E} = 0$ at equilibriums respectively. The above control does not vanish at dynamic attractors. Our aim, however, is not controlling the UPOs of unperturbed system existing at given parameter values, but rather the shift of a system into a region of desired behaviours. Energy (3) is changed so as to match energy of a desired state. For small oscillations, one can find amplitude ρ by substituting $x = \rho \sin \omega t$ into an averaged (over period T) energy change and solving equation

$$\langle \dot{E} \rangle = \frac{1}{T} \int_0^T \dot{E}(t)\,\mathrm{d}t = \frac{1}{T}\int_0^T \left(-\chi(x,\dot{x}) + F(t) + g(x,\dot{x})\right)\dot{x}\,\mathrm{d}t = 0. \tag{8}$$

Equation (8) describes the balance of dissipation and energy supply brought by damping, driving, and control forces. For general orbit defined by the infinite series of periodic modes, a fundamental mode as well as its harmonics should, in principle, be counted.

In this paper, we alter the feedback strength to adjust the oscillation energy to different levels. The above strategy does not require any computation of control signal and, hence, is applicable for control as well as identification of unknown systems.

Another strategy is based on a goal-oriented control of desired target. It can be applied in cases when the system equations are known or a desired target can be identified (say, extracted from the system time series). The amplitude of system's natural response is derived from equation

$$\frac{1}{T} \int_0^T \left(-\chi(x,\dot{x}) + F(t) \right) \dot{x} \, \mathrm{d}t = 0 \,. \tag{9}$$

Equation (9) describes the balance of dissipation and supply of system's intrinsic energy. For free self-sustained oscillations, this balance is supported entirely by nonlinear damping. To eliminate the natural response distortion imposed by the control, the following condition must be satisfied:

$$\frac{1}{T} \int_0^T \left(g(x,\dot{x}) \right) \dot{x} \, \mathrm{d}t = 0 \,. \tag{10}$$

For small oscillations, substitution of $g(x,\dot{x}) = k \tanh(\beta \dot{x}) \approx k(\beta \dot{x} - \frac{1}{3}\beta^3 \dot{x}^3)$ into (10) yields

$$\beta = \frac{2}{\rho \omega} \,. \tag{11}$$

Thus, the distortion can be minimized solely by tuning a perturbation shape. If $\rho \ll 1$, β should be sufficiently large so as to preserve the underlying natural response.

Control (6-7) does not depend on the type of functions $\chi(x,\dot{x})$, $\xi(x)$, and $F(t)$, and, hence, can be applied to linear and nonlinear oscillators, to regular and chaotic dynamics.

The approach can be easily generalized to a case of coupled oscillator networks (Tereshko et al., 2004b).

3. Controlling 2-D oscillators

3.1 Van der Pol oscillator

Consider the van der Pol oscillator with $\chi(x,\dot{x}) = (x^2 - \mu)\dot{x}$ and $\xi(x) = x$ controlled by feedback $g(\dot{x}) = k \tanh(\beta \dot{x})$. Linearizing the dynamic equation (1) in the vicinity of $x = 0$, one obtains the eigenvalues: $\lambda_1 = \left(\mu + k\beta - \sqrt{(\mu + k\beta)^2 - 4} \right)/2$ and $\lambda_2 = \left(\mu + k\beta + \sqrt{(\mu + k\beta)^2 - 4} \right)/2$. At $\mu > 0$ and $k < 0$, the perturbation with $k < -(1/\beta)\mu$ or $\beta > (1/|k|)\mu$ stabilizes the unstable equilibrium. Thus, two control strategies can be applied: (i) altering the perturbation magnitude; (ii) reshaping the perturbation. When $\beta \to \infty$, $\tanh(\beta \dot{x}) \to \mathrm{sign}(\dot{x})$. The energy change caused by the control yields $g(\dot{x})\dot{x} = k\,\mathrm{sign}(\dot{x})\,\dot{x} = k\,|\dot{x}|$. This strategy corresponds to maximizing the rejection (injection) of the oscillation energy and is, in fact, the first approximation of optimal control for a van der Pol oscillator with small dissipation (Kolosov, 1999).

3.2 Forced two-well Duffing oscillator

To analyze controlling chaotic oscillators, consider the forced two-well Duffing oscillator with negative linear and positive cubic restoring terms:

$$\ddot{x} + e\dot{x} - x + x^3 = b \cos \omega t + k \tanh(\beta \dot{x}) \,. \tag{12}$$

In unperturbed system, at $e = 0.3$, $\omega = 1.2$, and $b < 0.3$, the "particle" become trapped into other left or right potential well oscillating around $x = -1$ and $x = 1$ respectively (or tending to these stationary states when $b = 0$). At $b \gtrsim 0.3$, the particle is able to escape the wells, its irregular wandering between two potential wells corresponding to chaotic oscillations. Taking
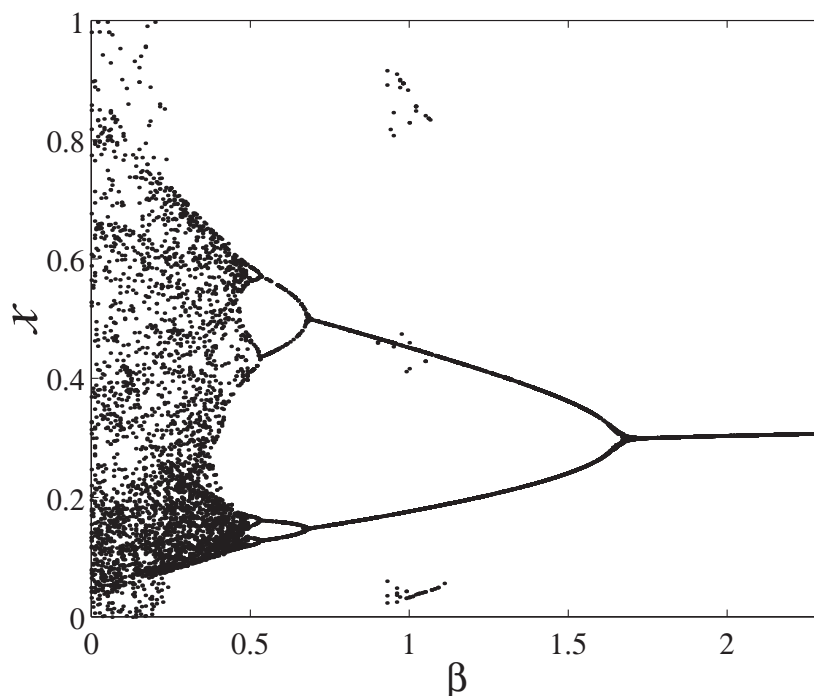
Fig. 1. Bifurcation diagram of oscillator (12) at $e = 0.3$, $\omega = 1.2$, $b = 0.31$, and $k = -0.06$.

the linear approximation $\tanh(\beta\dot{x}) \approx \beta\dot{x}$, obtain $\dot{E} = \big((-e + k\beta)\dot{x} + b\cos\omega t)\big)\dot{x}$. At small β's, the control action is, thus, equivalent to linear adjustment of the oscillator damping. With increasing β, the influence of the perturbation nonlinearity respectively increases.

Let us fix the amplitude k and change only the perturbation slope β. This induces the double action: (i) reshaping the perturbation, and (ii) changing its effective amplitude k_{ef}. Increasing the slope leads to the increase of k_{ef} (it changes from 0 to k when β changes from 0 to ∞). As a result, when $k < 0$ the sequential stabilization of orbits of the period-doubling cascade occurs in the reverse order (Fig. 1). These orbits are stabilized at relatively small β and k. Around $\beta = 1$, the coexisting orbits multiple of period 3 appear. They can be eliminated by the slow modulation of either k or h. The similar effect of reverse period-doubling is reached at increasing e. However, suppressing the oscillations (to a state where the trajectory remains in the vicinity of either 1 or -1) occurs only at extremely high e. Hereupon, the system dynamics becomes overdamped, which requires extremely long transitional times. In contrast, the perturbations with large β effectively suppress the oscillations when k remains relatively small (Fig. 2). Note, the requirement for large β follows from condition (11): when $\rho \to 0$, $\beta \to \infty$. Unlike stabilization of stationary points in unforced oscillators, the system trajectory slightly deviates around the controlled point (with the amplitude less than 10^{-3} in Fig. 2), and the control, hence, does not vanish there. This happens because stationary points in forced oscillators are not the invariants of dynamics and become these only at zero forcing. Figure 3 demonstrates the entrainment between the feedback force at very small and large β's, when stabilizing the period-1 orbit and the stationary point respectively, and the driving force waveforms. The larger β the better the perturbation force waveform fits (in anti-phase) the driving force to suppress the latter. Tuning the phase and the shape of perturbation to their driving force counterparts is equivalent to combining the driving and the perturbation forces into the one effective force $F_{ef} = (b + k)\cos\omega t$.

Changing the perturbation phase on the opposite one leads to the increase of the averaged oscillation energy allowing the UPOs corresponding to the higher values of energy (2) be
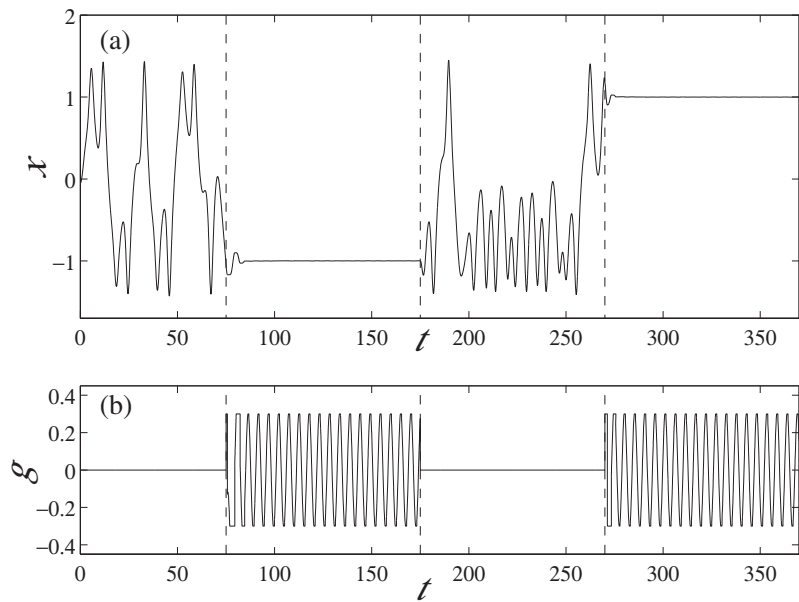
Fig. 2. Dynamics of (a) the state variable and (b) the control perturbation of oscillator (12) at $e = 0.3$, $\omega = 1.2$, $b = 0.31$, $k = -0.3$, and $\beta = 5000$.
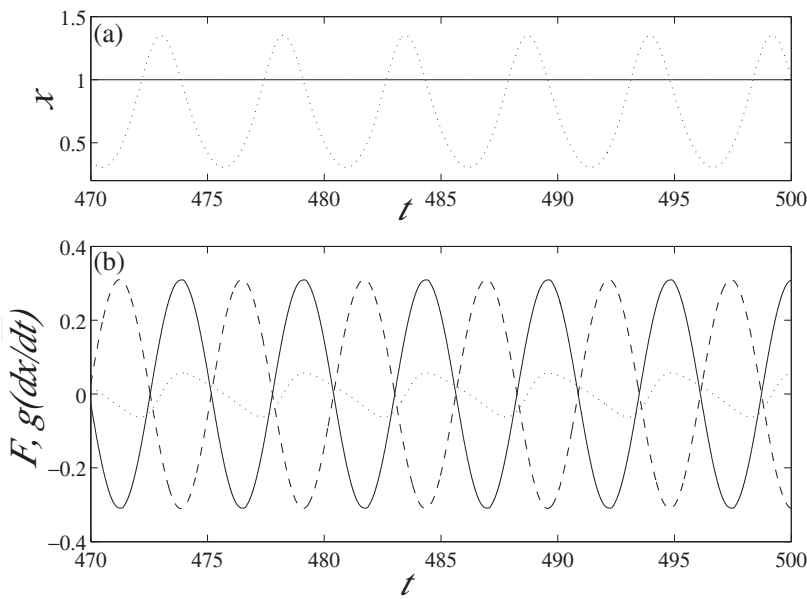

Fig. 3. Dynamics of (a) the state variable at $\beta = 5000$ and $k = -0.31$ (solid line); $\beta = 0.01$ and $k = -9$ (dotted line), and (b) the control perturbation at $\beta = 5000$ and $k = -0.31$ (solid line); $\beta = 0.01$ and $k = -9$ (dotted line), and the driving force (dashed line) of oscillator (12). For all graphs, $e = 0.3$, $\omega = 1.2$, and $b = 0.31$.
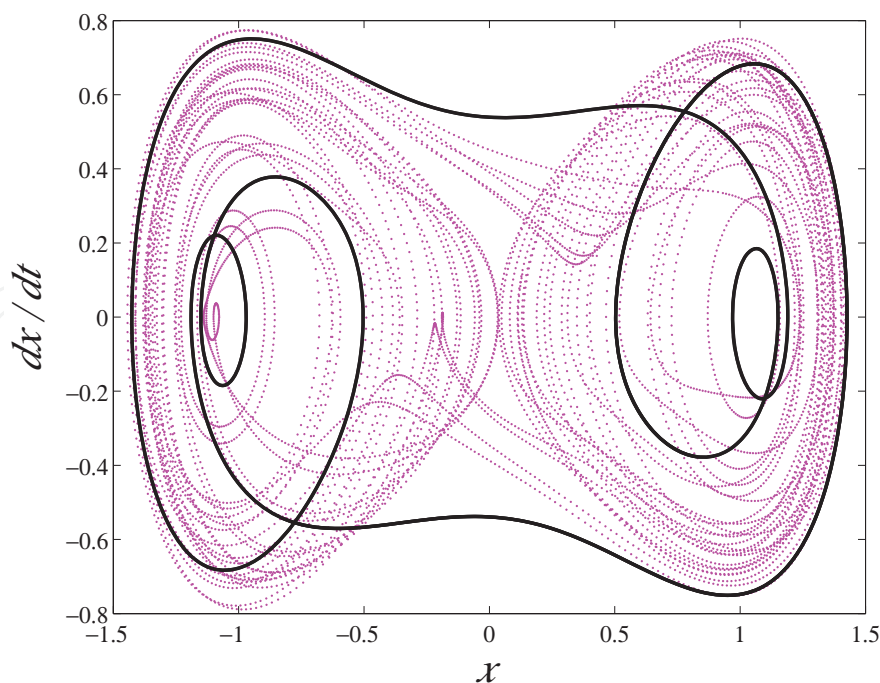
Fig. 4. Phase space of oscillator (12) at $e = 0.3$, $\omega = 1.2$, $b = 0.31$, $\beta = 2$, and $k = 0$ (grey dotted line); $k = 0.06$ (bold solid line).

stabilized. Figure 4 demonstrates the stabilization of period-5 orbit. The similar strategy can destabilize the initially stable system by shifting it to the chaotic regions.

3.3 Forced van der Pol oscillator
Controlling chaotic oscillators with nonlinear damping shows the clearly different scenarios of the control. Let us analyze the forced van der Pol oscillator:

$$\ddot{x} + e(x^2 - \mu)\dot{x} + x = b\cos\omega t + k\tanh(\beta\dot{x}) . \tag{13}$$

In the unperturbed system, no regularity is observed at $e = 5$, $\mu = 1$, $b = 5$ and $\omega = 2.463$ (Fig. 5(a)). At small enough β, obtain $\dot{E} = \left(- e(x^2 - (\mu + e^{-1}k\beta))\dot{x} + b\cos(\omega t)\right)\dot{x}$. Unlike the previous case, even a weak control perturbation changes nonlinearly the oscillator damping. One can expect the markedly different manifestations of the control at small and large β, respectively. Indeed, the control with $k < 0$ decreases the negative damping term, which leads to stabilization of the period-3 and the period-1 orbits (Fig. 5(b)). These orbits are different from the orbits stabilized by decreasing the driving force amplitude. We compared the stabilized orbits and their unperturbed counterparts. To stabilize the period-1 orbit, the control perturbation induces the shift of μ to $\mu' = \mu - e^{-1}k\beta$ (see Fig. 5(b)). As predicted by the theory, the stabilized orbit and the unperturbed orbit that corresponds to this shift coincide. For orbits with more complicated shapes, the stabilized orbits trace closely their unperturbed counterparts.

With the increase of β, the control perturbation begins to affect the driving force term. Figure 5(c) demonstrates the stabilization of period-5 orbit corresponding to the lower amplitudes of driving force.
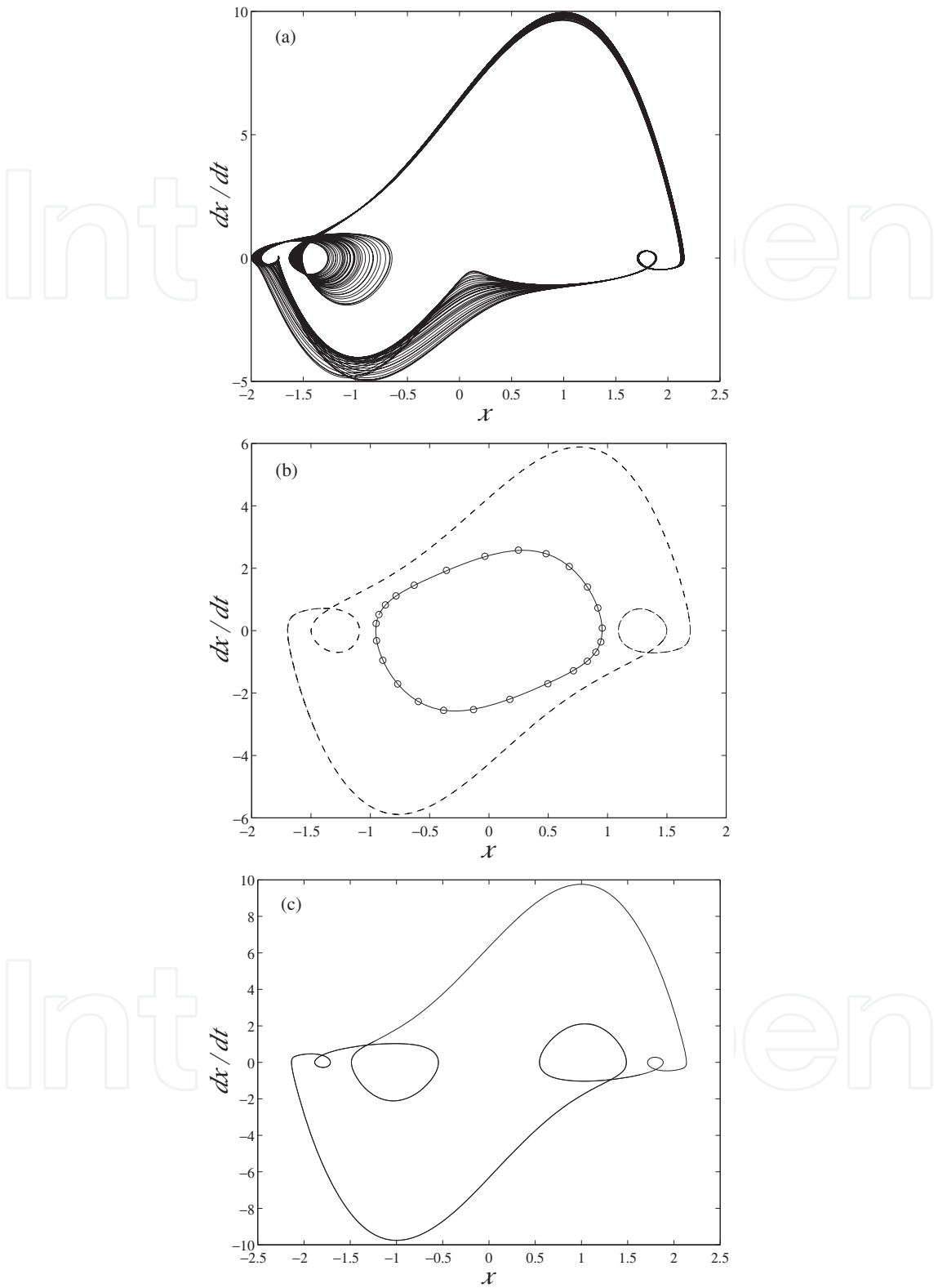
Fig. 5. Phase space of oscillator (13) at $e = 5$, $\mu = 1$, $\omega = 2.463$, $b = 5$, and (a) $k = 0$; (b) $\beta = 0.1$, and $k = -20$ (dashed line); $k = -40$ (solid line); circles indicate the period-1 cycle of the unperturbed system at $e = 5$, $\mu = 0.2$, $\omega = 2.463$, and $b = 5$; (c) $\beta = 3$, and $k = -0.13$.
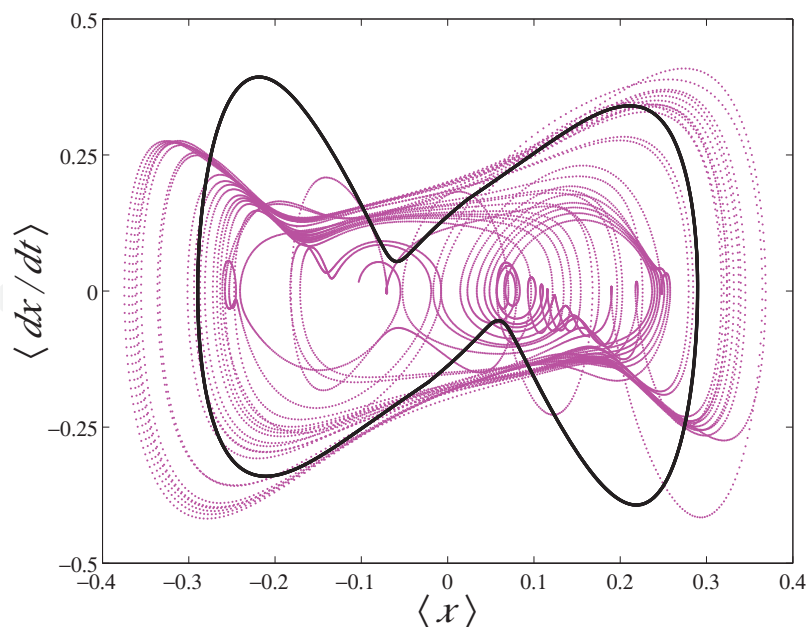
Fig. 6. Phase space of oscillator network (14) for the averaged trajectory ($\langle x \rangle = \frac{1}{n} \sum_{i=1}^{n} x$ and $\langle \dot{x} \rangle = \frac{1}{n} \sum_{i=1}^{n} \dot{x}$) at $e = 0.18$, $\nu = 8$, $\omega = 1.02$, $b = 0.35$, $\frac{1}{n}(\alpha_1, \alpha_2, .., \alpha_n) = $ (1.7861, -2.1131, 0.2561, 2.2297, -1.3585, -0.6648, 1.1977, 0.2451, -2.2229, 0.4282), $n = 10$ and $k = 0$ (grey dotted line); $k = -0.18$ (solid line). $j = \arg \left\{ \min \left(|\alpha_1|, |\alpha_2|, .., |\alpha_n| \right) \right\} = 8$, which implies the perturbation to be applied to 8th oscillator.

3.4 Coupled oscillators

Consider controlling the network of n oscillators coupled via the mean field. As the network element, take the forced van der Pol-Duffing oscillator, an oscillator with the van der Pol nonlinear damping and the modified Duffing restoring force containing only the cubic term. This oscillator describes the dynamics of nonlinear circuit (Ueda, 1992). Let us assume that the oscillators are identical but their coupling strengths are randomly varied, and only single element of the network is subjected to the control. The oscillator with the weakest coupling strength is least affected by the mean field, and, hence, is most preserving own intrinsic dynamics. We apply the control to this oscillator. The oscillator network equations, thus, read

$$\ddot{x}_j + e(\nu x_j^2 - 1)\dot{x}_j + x_j^3 + \alpha_j \frac{1}{n} \sum_{i=1}^{n} x_i = b \cos \omega t + k \tanh(\beta \dot{x})$$

$$\ddot{x}_l + e(\nu x_l^2 - 1)\dot{x}_l + x_l^3 + \alpha_l \frac{1}{n} \sum_{i=1}^{n} x_i = b \cos \omega t \tag{14}$$

where $j = \arg \left\{ \min \left(|\alpha_1|, |\alpha_2|, .., |\alpha_n| \right) \right\}$, $l = 1, 2, .., n$, $l \neq j$.

For single oscillator, the dynamics is chaotic at $e = 0.2$, $\nu = 8$, $\omega = 1.02$, and $b = 0.35$ (Ueda, 1992). Coupling 10 chaotic oscillators by the connections with strengths varied randomly according to the Gaussian distribution (with the mean equal to 0, and the variance and the standard deviation equal to 1) produces various dynamics. Figure 6 demonstrates the averaged trajectory of the network that reveals all futures of chaotic behaviour. The perturbation decreasing the averaged oscillation energy, being applied to the most weakly connected oscillator, stabilizes the network dynamics. Controlling, in opposite, the most

strongly connected oscillator leads to the similar results requiring, however, much larger control amplitudes.

We performed the simulations of higher dimensional networks. For 50 oscillator network with random normally distributed coupling strengths, the control perturbation applied to the most weakly coupled oscillator is found to stabilize the dynamics.

4. Controlling 3-D oscillators

4.1 Colpitts oscillator

The chaotic attractors have been observed in several electronic circuits. One of such circuit is the Colpitts oscillator (Baziliauskas, 2001; De Feo, 2000; Kennedy, 1994). It consists of a bipolar junction transistor (the circuit active nonlinear element) and a resonant L-C circuit. The oscillator is widely used in electronic devices and communication systems.

The Colpitts oscillator dynamics can be described by the following dynamical system (Baziliauskas, 2001):

$$\begin{aligned} \dot{x} &= y - f(x) \\ \dot{y} &= c - x - by - z \\ \varepsilon\dot{z} &= y - d \end{aligned} \tag{15}$$

where function

$$f(x) = \begin{cases} -a(z+1), & z < -1, \\ 0, & z \geqslant -1, \end{cases}$$

dimensionless variables x and z correspond to circuit's capacitor voltages, and variable y corresponds to circuit's inductor current. a, b, c, d are the dimensionless parameters. This model is equivalent to the so-called ideal model of the circuit (De Feo, 2000). It maintains, however, all essential features exhibited by the real Colpitts oscillator. For $z < -1$, the transistor works in its forward-active region, while for $z \geqslant -1$, it is cut-off.

Substituting $y = \varepsilon\dot{z} + d$ to the second equation of (16), obtain

$$\begin{aligned} \varepsilon\ddot{z} + \varepsilon b\dot{z} + z &= c - bd - x \\ \dot{x} &= -f(x) + \varepsilon\dot{z} + d \, . \end{aligned} \tag{16}$$

To apply the above approach, one need to add feedback $g(\dot{x})$ to the first equation of system (16). For the above oscillator, the change of energy (2) caused by this control yields $\dot{z}g(\dot{z})$. If $g(\dot{z})$ takes form (6-7), the latter term always provides the increase (decrease) of the oscillation energy for positive (negative) perturbation magnitudes. We, thus, consider $g(\dot{z}) = k \tanh(\beta\dot{z})$. Taking $\dot{z} = \frac{1}{\varepsilon}(y - d)$, obtain the control feedback to apply to the second equation of system (16):

$$g(y) = k \tanh\left(\frac{1}{\varepsilon}\beta(y - d)\right) . \tag{17}$$

Perturbation (17) is specially tuned to control the equilibrium of system (16). Figure 7 demonstrates the latter. k is chosen to be negative, which results in decreasing the averaged oscillation energy.

Note, the stationary point exists only in the forward-active region. Unlike, the periodic orbit trajectories spend most of their times in the cut-off region. The circuit oscillations are balanced, thus, not around the above stationary point but rather around the total collector voltage equilibrium. The latter is proportional to $x + z$. Let us consider $\varepsilon = 1$ and define $w = x + z$. In
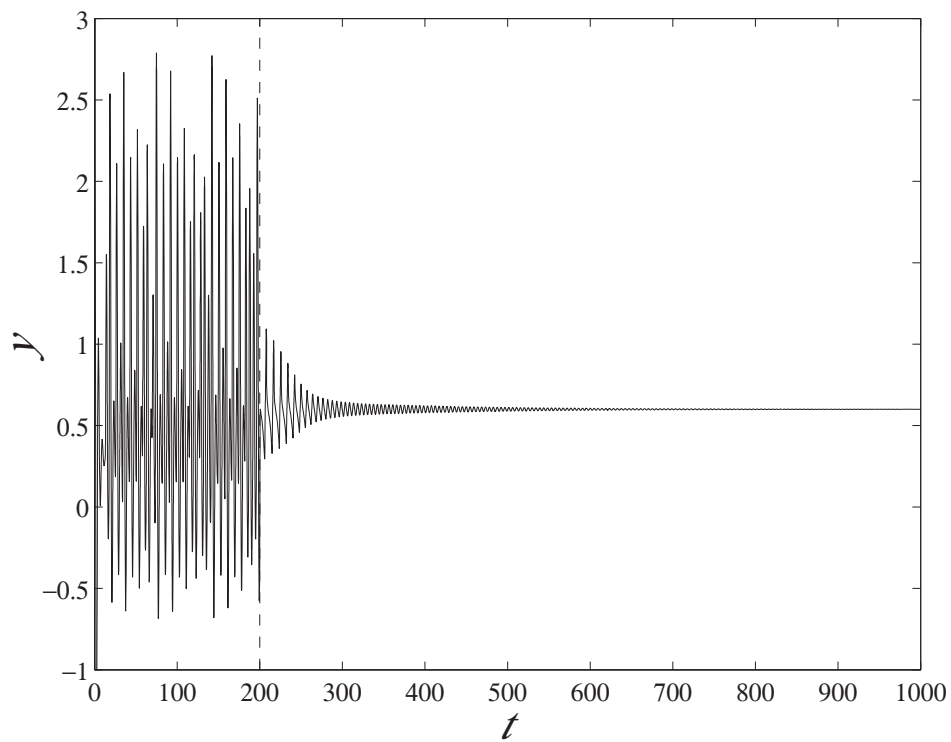
Fig. 7. Dynamics of the state variable of oscillator (16) at $\varepsilon = 1$, $a = 30$, $b = 0.8$, $c = 20$, $d = 0.6$, $\beta = 10$, and $k = 0$ ($t < 200$); $k = -1.6$ ($t \geqslant 200$). Dashed line indicates the time of starting the control.
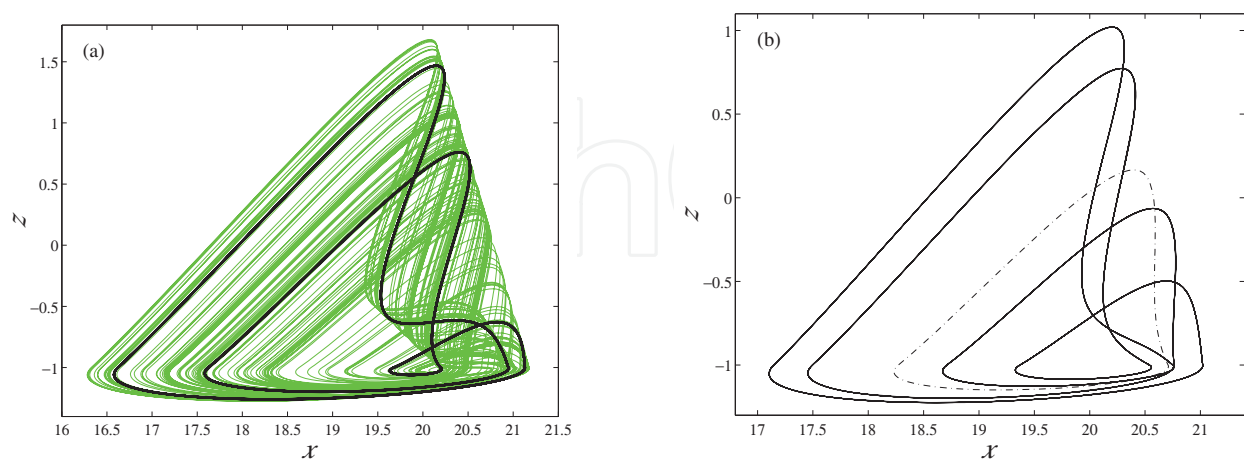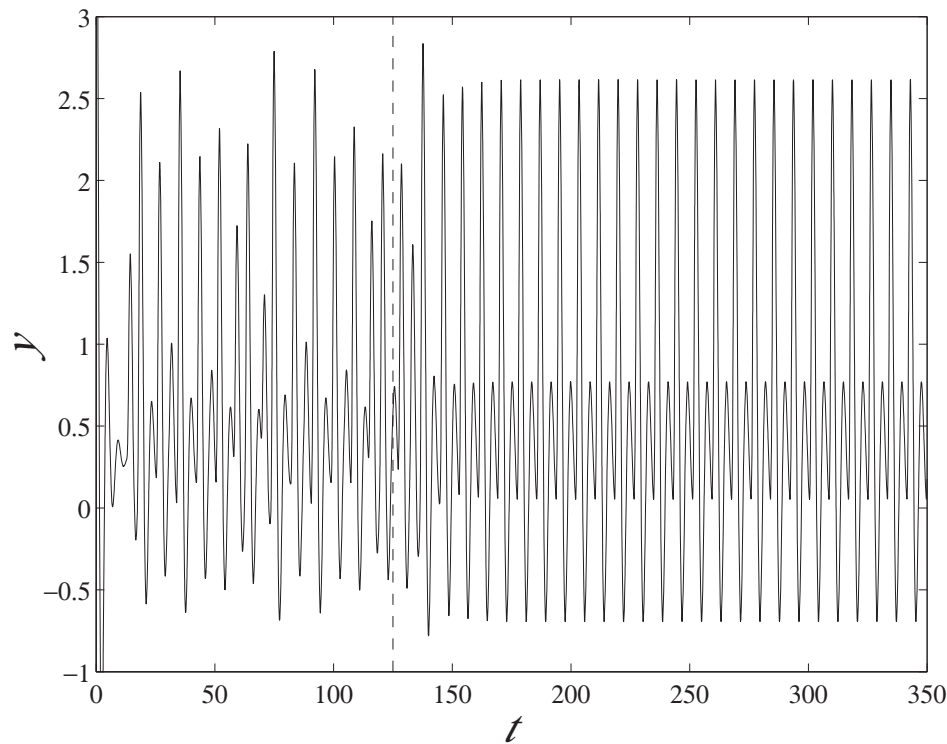

Fig. 8. Phase space of oscillator (16) at $\varepsilon = 1$, $a = 30$, $b = 0.8$, $c = 20$, $d = 0.6$, $\beta = 10$, and (a): $k = 0$ (grey line); $k = -0.009$ (bold black line); (b): $k = -0.012$ (solid line); $k = -0.24$ (dot-dashed line)

Fig. 9. Dynamics of the state variable of oscillator (16) at $\varepsilon = 1$, $a = 30$, $b = 0.8$, $c = 20$, $d = 0.6$, $\beta = 10$, and $k = 0$ ($t < 125$); $k = 0.08$ ($t \geqslant 125$). Dashed line indicates the time of starting the control.

the cut-off region, the summation of first and third equations of system (16) yields $\dot{w} = 2y - d$. Substitution of $y = \frac{1}{2}(\dot{w} + d)$ to the second equation of system (16) results in the following dynamics of the total collector voltage:

$$\ddot{w} + b\dot{w} + 2w = 2c - bd . \tag{18}$$

Perturbation $g(\dot{w})$ satisfying conditions (6-7) being applied to oscillator (18) results in the following:

$$g(y) = k \tanh \left(\beta(y - \frac{d}{2}) \right) \tag{19}$$

To control circuit's periodic orbits, the second equation of system (16) should be exposed to the latter feedback.

Figures 8 and 9 demonstrate controlling the oscillator periodic orbits. At $k = 0$, the system exhibits chaotic oscillations (Fig. 8(a), grey line). Let us apply the feedback that decreases the oscillation energy. Strengthening its force, one sequentially stabilizes the orbits corresponding to the windows of chaotic attractor and then the period-doubling orbits of main cascade in their reverse order. At $k \simeq -0.009$, one obtains the period-3 orbit corresponding to the largest window of chaotic attractor (Fig. 8(a), bold black line). The period-8, -4, -2, and -1 orbits are stabilized at $k \simeq -0.11, -0.12, -0.14, -0.22$ respectively. Figure 8(b) demonstrates the stabilized period-4 (solid line) and the period-1 (dot-dashed line) orbit respectively.

Increasing the oscillation energy leads to the stabilization of orbits corresponding to these energy levels. As example, Fig. 9 demonstrates the stabilization of so-called 2-pulse orbit.

We also considered a chain (ring) of 10 Colpitts oscillators with the diffusion-type couplings (with coupled emitters and collectors of the circuit transistor (Baziliauskas, 2001)). Different UPOs were stabilized with control perturbations applied to only single oscillators.

4.2 Chua's oscillator

Let us consider controlling a system that produces two major mechanisms of chaotic behaviour in continuous systems — the Rössler and the Lorenz types. This system is the Chua's circuit, an autonomous electronic circuit modelled by equations (Chua et al., 1986; Wu, 1987):

$$
\begin{aligned}
\dot{x} &= a(y - f(x)) \\
\dot{y} &= x - y + z + g(y) \\
\dot{z} &= -by
\end{aligned}
\tag{20}
$$

where function $f(x) = m_1 x + \frac{1}{2}(m_0 - m_1)(|x+1| - |x-1|)$, a is the bifurcation parameter, and $g(y)$ is the control perturbation.

We take $b = 15$, $m_0 = -\frac{1}{7}$, and $m_1 = \frac{2}{7}$. With increasing a in the unperturbed system, the steady states, ($x^{(s)} = p, y^{(s)} = 0, z^{(s)} = -p$) and its symmetric image ($x^{(s)} = -p, y^{(s)} = 0, z^{(s)} = p$), where $p = \frac{(m_1 - m_0)}{m_1}$, become unstable, and a limit cycle arises through the Andronov-Hopf bifurcation. Further increasing the bifurcation parameter leads firstly to the Rössler-type chaos through the period-doubling cascade, and then to merging two Rössler bands and to forming the double scroll attractor (Chua et al., 1986). The oscillation amplitude grows as α increases.

Substituting $y = -\frac{\dot{z}}{b}$ to the second equation of (20) and assuming $g(y)$ to be the odd function, obtain

$$
\ddot{z} + \dot{z} + bz = -bx + bg(\frac{\dot{z}}{b})
$$

$$
\dot{x} = a(-\frac{\dot{z}}{b} - f(x)) .
\tag{21}
$$

For oscillator (21), the change of energy caused by the control yields $b\dot{z}g(\frac{\dot{z}}{b})$. If $g(\frac{\dot{z}}{b})$ takes form (6-7), the latter term always provides the increase (decrease) of the oscillation energy for the positive (negative) perturbation magnitudes. We, thus, consider $g(\frac{\dot{z}}{b}) = k \tanh(\beta\frac{\dot{z}}{b})$. Taking into account that $\dot{z} = -by$ and considering the limit $\beta \to \infty$, obtain the following control term:

$$
g(y) = k \, \mathrm{sign}(y) .
\tag{22}
$$

At negative k, perturbation (22) reduces the oscillation energy. The increase of perturbation amplitude recovers all lower energy repellors of system (20). Figure (10) demonstrates the bifurcation diagram of system (20) at $a = 9$. Here, we considered only the trajectories corresponding to the right hand wing of the attractor. The unperturbed system exhibits the chaotic behaviour that corresponds to the screw-type chaos of the Rössler band attractor. At $0.0083 \lesssim k \lesssim 0.0097$, the orbits of period $3 \cdot 2^i, i = 0, 1, 2...$ (in the reverse order beginning with the highest period) are stabilized. These orbits correspond to the largest window of the Rössler band. As known, this window separates the two different types of Rössler chaos in Chua's circuit, the screw-type chaos and the spiral chaos. At the higher amplitudes of control perturbation, the behaviour becomes converted to the spiral chaos featuring, thus, the control of chaotic repellor. The further increase of control amplitude leads firstly to the sequential

stabilization of 2^i, $i = 0, 1, 2...$ orbits (these UPOs are controlled at $0.0193 \lesssim k \lesssim 0.0392$, again, in the reverse order beginning with the highest period orbit) and finally to the stabilization of the steady state corresponding to the controlled band (Fig. 11). In the latter case, the perturbation evolves to the high-frequency periodic oscillations controlling the stationary state. One can draw a clear parallel between this case and the stabilization of unstable equilibrium in a rapidly oscillating field, which is the classical example of physics (Landau & Lifshitz, 1976).

The last example demonstrates the self-tuning nature of given control. Indeed, to stabilize the periodic orbits, the perturbation evolves to the required resonant one. Unlike, when controls the chaotic repellors, the perturbation switches chaotically between $-k$ and k.
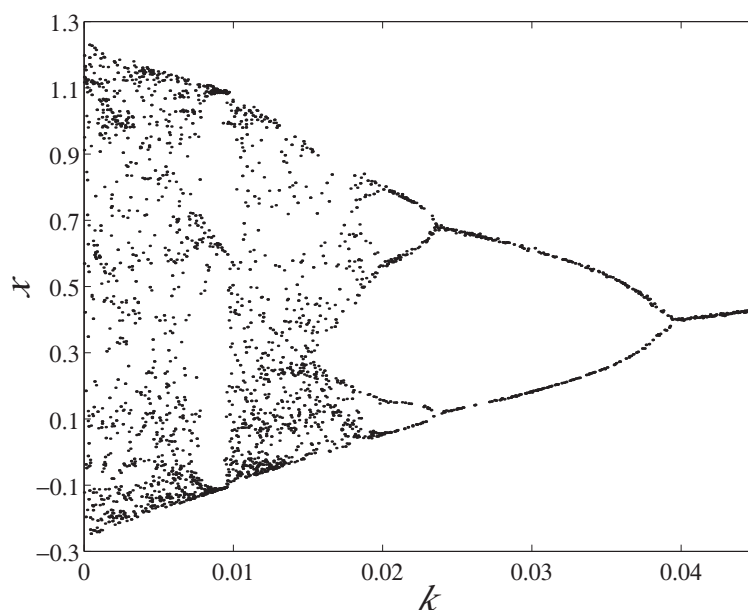
Fig. 10. Bifurcation diagram of perturbed Chua's circuit (20) at $b = 15$, $m_0 = -1/7$, and $m_1 = 2/7$, $a = 9$.

In the nonchaotic regimes, one can apply the similar strategy. Consider, for example, $a = 8$, which corresponds to the period-1 oscillations. Taking positive k and increasing it, the system will be driven to the higher energy states. As a result, all these states can be controlled, namely: the period-doubled orbits, the repelling Rössler band and double scroll, and the UPOs of latter repellors.

Consider now the double scroll attractor ($a = 10$, Fig. 12(a)). At negative k, strengthening the perturbation decreases the oscillation energy, allowing to control the lower energy repellors. Figure 12(b) illustrates the control of UPO corresponding to a window of the double scroll. At the higher amplitude of control perturbation, one observes the reverse bifurcation of the double scroll birth when the trajectories from two loci diverge and form two separate odd-symmetric Rössler bands. Depending on the locus where the control is turned on, one or another band can be controlled. Figure 12(c) illustrates controlling the right-hand Rössler band. Increasing the control amplitude, one stabilizes sequentially the period-doubling orbits in their reverse order. Fig. 12(d) shows controlling the period-4 orbit. The further increase of control amplitude leads to the stabilization of steady states. However, the unstable steady states can be controlled by a weaker perturbation, if the control is turned on in the vicinity of
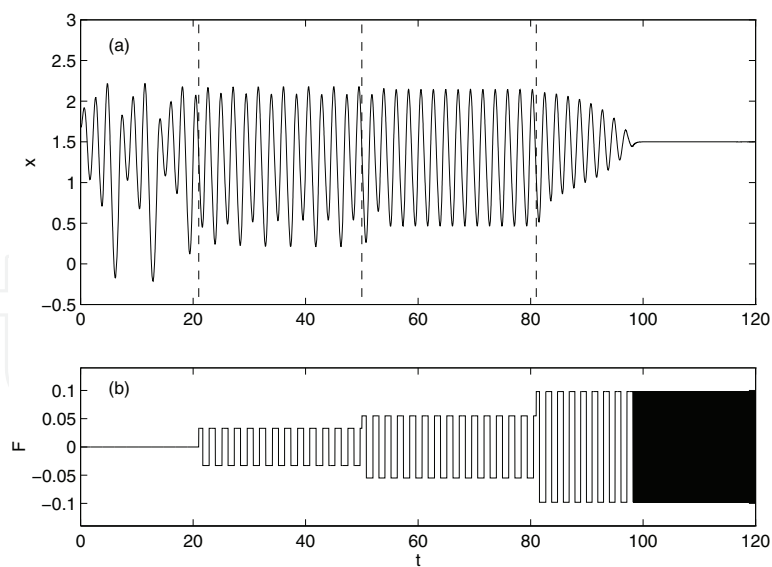
Fig. 11. Dynamics of (a) perturbed Chua's circuit (20) and (b) its control perturbation at $b = 15$, $m_0 = -1/7$, $m_1 = 2/7$, $a = 9$, and $k = 0$ ($0 \leq t < 21$); $k = -0.033$ ($21 \leq t < 50$); $k = -0.055$ ($50 \leq t < 81$); $k = -0.098$ ($t > 81$).
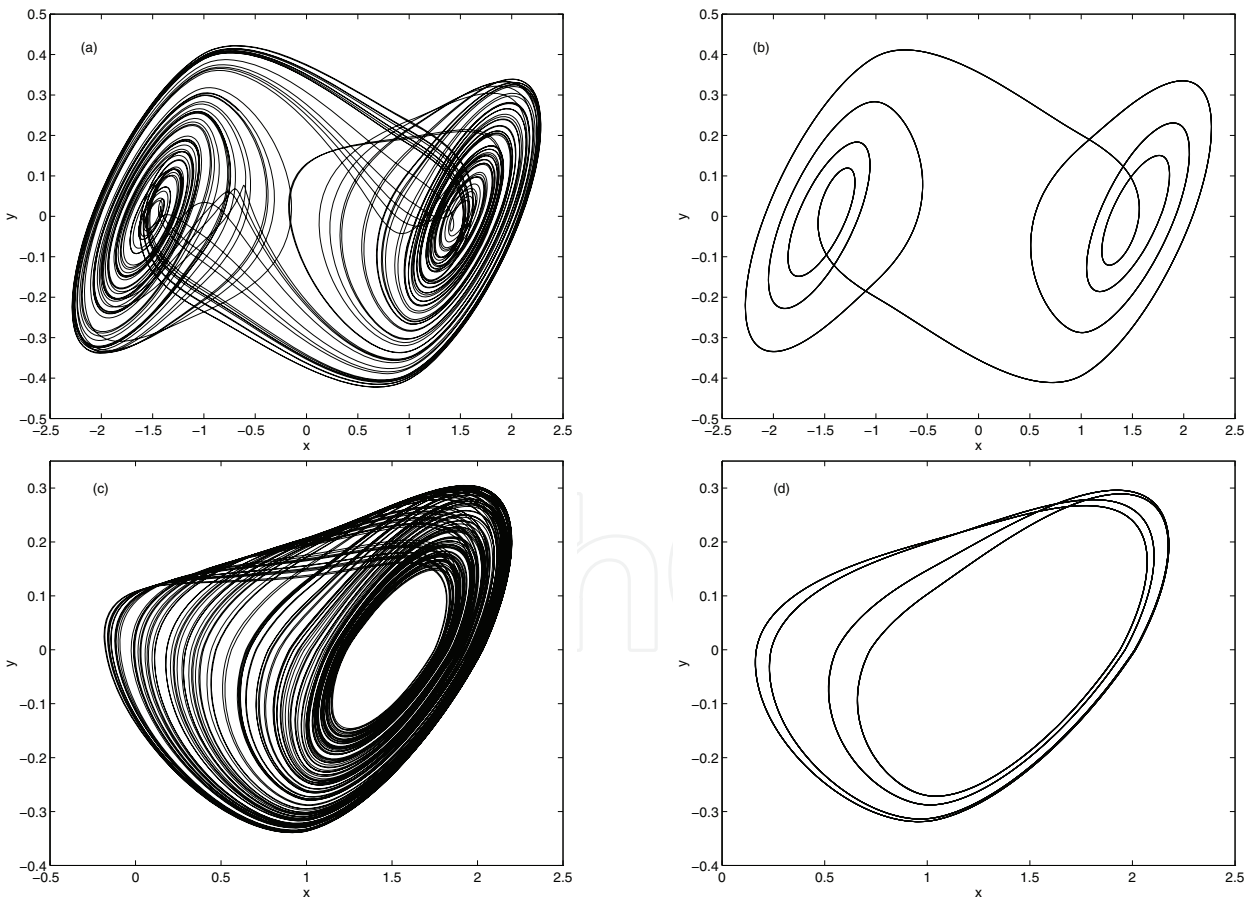

Fig. 12. State space of perturbed Chua's circuit (20) at $b = 15$, $m_0 = -1/7$, $m_1 = 2/7$, $a = 10$, and (a) $k = 0$; (b) $k = -0.0085$; (c) $k = -0.068$; (d) $k = -0.085$.

these states. To control the UPOs corresponding to the lower energy levels, the perturbation decreasing the oscillation energy, i.e. one with the positive k, should be applied.

5. Controlling reaction-diffusion media

The above strategy can be generalized to control the pattern dynamics in the spatially-extended systems. Consider a general reaction-diffusion system:

$$\frac{\partial u}{\partial t} = \xi(u) + \frac{\partial^2 u}{\partial r^2} \,. \tag{23}$$

This equation possesses a special solution of the form $u = u(r - ct)$, where c is the wave speed, called a travelling wave (23). Taking new variable $\varrho = r - ct$, obtain

$$\ddot{u} + c\dot{u} + \xi(u) = 0 \tag{24}$$

where all derivatives are taken over ϱ. Perturbation (6-7) is able to effectively increase or decrease the oscillation energy of travelling wave enhancing or suppressing the latter respectively.

Let us consider an excitable medium. It is characterized by the existence of the only equilibrium, the resting state, yet being perturbed the system trajectory is able to spend a substantial time outside of the equilibrium, in the firing state. Let us augment equation (23) with new "recovery" variable v that allows the system dynamics to return to its resting state:

$$\dot{v} = \psi(u, v) \tag{25}$$

Assuming the existence of travelling wave solution, throughout we consider the following system:

$$\ddot{u} + c\dot{u} + \zeta\big(\xi(u) + \varphi(u, v)\big) = 0$$
$$\dot{v} + \frac{1}{c}\psi(u, v) = 0 \,. \tag{26}$$

Typically, $\varphi(u, v)$ and $\psi(u, v)$ are the linear combinations of u and v, and $\xi(u, v)$ is a nonlinear function. The most known examples of nonlinear kinetics in the excitable media are represented by functions $\xi(u) = u - \frac{1}{3}u^3$ and $\xi(u) = \Theta(u - \delta)$ where Θ is the Heaviside step function. The latter is equal to 1 when v exceeds the threshold value δ, and 0 otherwise. These choices belong to the classical FitzHugh-Nagumo (FitzHugh, 1961) and Rinzel-Keller (Rinzel & Keller, 1973) models respectively.

To control the travelling waves, we apply the control perturbation to the right-hand side of the first equation of system (26):

$$\ddot{u} + c\dot{u} + \zeta\big(\xi(u) + \varphi(u, v)\big) = k \tanh(\beta \dot{u}) \,. \tag{27}$$

The latter is, in fact, the introduction of some form of nonlinear damping into the system. For small β, the linear approximation yields $\tanh(\beta \dot{u}) \approx \beta \dot{u}$, and the control reduces to the adjustment of the travelling wave speed:

$$\ddot{u} + (c - k\beta)\dot{u} + \zeta\big(\xi(u) + \varphi(u, v)\big) = 0 \,. \tag{28}$$

The distributed version of the above control can be directly applied to system (23), viewing it as a spatially distributed overdamped oscillator. Note, ϱ is the function of both t and r giving the opportunity for the two types of control. The first type reads:

$$\frac{\partial u}{\partial t} = \xi(u) + \frac{\partial^2 u}{\partial r^2} + k(r,t)\tanh\left(\beta\frac{\partial u}{\partial t}\right). \tag{29}$$

Generally, k is the function of r and t. Throughout, however, we demonstrate the efficiency of the spatially localized perturbations with the constant in time amplitudes. In the limit of small β and constant k, the control reduces to the simple timescale and diffusion coefficient adjustments:

$$\frac{\partial u}{\partial t} = \frac{1}{(1-k\beta)}\left(\xi(u) + \frac{\partial^2 u}{\partial r^2}\right). \tag{30}$$

Unlike the adjustment of the travelling wave speed in (28), the above one affects the whole right-hand side of the equation and, hence, must be bounded to $k\beta < 1$ (unless one intends to drastically modify the system).

The second type of control reads:

$$\frac{\partial u}{\partial t} = \xi(u) + \frac{\partial^2 u}{\partial r^2} + k(r,t)\tanh\left(\beta\frac{\partial u}{\partial r}\right). \tag{31}$$

Here, the last term is nothing but the nonlinear flow, which, in the limit of small β, tends to its linearized version.

When suppressing the travelling waves in excitable media, after some period of exposition, the control can be switched off. Indeed, the rest state is the stable equilibrium here, and the perturbation should only be imposed while the trajectory is out of its basin of attraction.

Below, consider the above control on the examples of two models of excitable reaction-diffusion media.

5.1 Distributed FitzHugh Nagumo model

This system is the approximation of Hodgkin-Huxley model (Hodgkin & Huxley, 1952) of the propagation of voltage pulses along a nerve fibre. The dynamics is described by the system of coupled equations (Scott, 1975):

$$\frac{\partial u}{\partial t} = u - \frac{1}{3}u^3 - v + \iota + \frac{\partial^2 u}{\partial r^2}$$

$$\frac{\partial v}{\partial t} = \alpha(u - av + b) \tag{32}$$

where u represents the local electric potential across the cell membrane and v represents the conductivity of the voltage-sensitive ionic channels. Parameters ϱ, a and b represent the membrane's current, radius and resistivity respectively, and parameter α constitutes the temperature factor.

5.1.1 Excitable regime

When looking for a travelling wave solution, the problem reduces to solving the ODEs equations:

$$\ddot{u} + c\dot{u} + u - \frac{1}{3}u^3 - v + \iota = 0$$
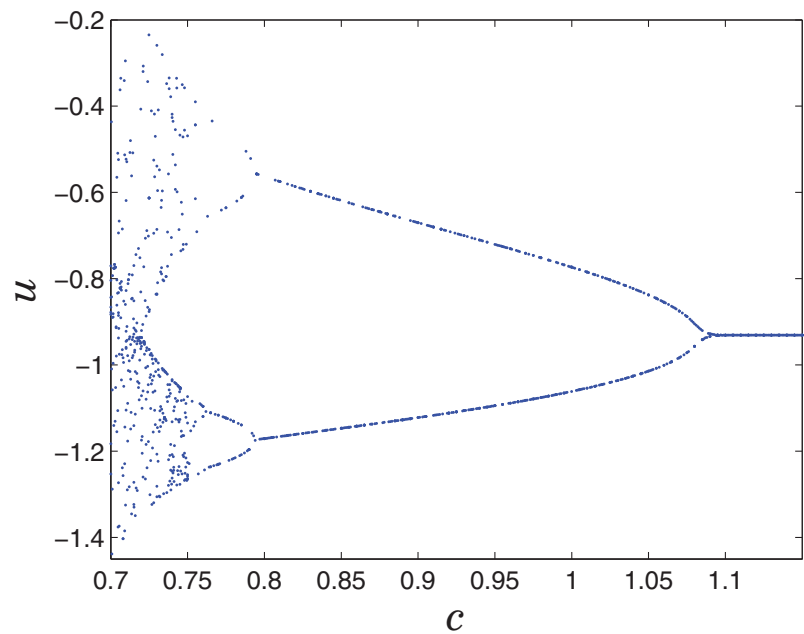
$$\dot{v} = -\frac{\alpha}{c}(u - av + b). \tag{33}$$

Fig. 13. Bifurcation diagram of system (33) at $a = 0.5$, $b = 0.6$, $\alpha = 0.1$, and $\iota = 0$.

The forced-free system, i.e. one with $\iota = 0$, demonstrates the transition to chaos with the decrease of c (Fig. 13). Obviously, the linear damping control (28) will stabilize the dynamics. More efficient, however, to utilize the nonlinearity of sigmoid-type control perturbation as in (27). Fig. 14 illustrates the control of various period orbits by the tanh-perturbation.

The similar strategy is applied to the periodically driven system. When the membrane is subjected to the periodic current, i.e. $\iota = \rho \cos(\omega t)$, system (33) demonstrates the chaotic behaviour as well as its driven-free analogue (Rajesekar & Lakshmanan, 1994). Fig. 15 illustrates the control of above system.

5.1.2 Oscillatory regime

Fig. 16 illustrates controlling the system in the oscillatory mode applying the linearized version of control (31). Depending on the sign of control perturbation, one can either increase the oscillation frequency or suppress the oscillations.

5.2 Kahlert-Rössler model

The Kahlert-Rössler model is a variant of the Rinzel-Keller system (Rinzel & Keller, 1973) of the nerve conduction (Kahlert & Rössler, 1984):

$$\frac{\partial u}{\partial t} = \mu\big(-u + \Theta(u - \delta) + v - \gamma\big) + \frac{\partial^2 u}{\partial r^2}$$
$$\frac{\partial v}{\partial t} = -\epsilon u + v \tag{34}$$

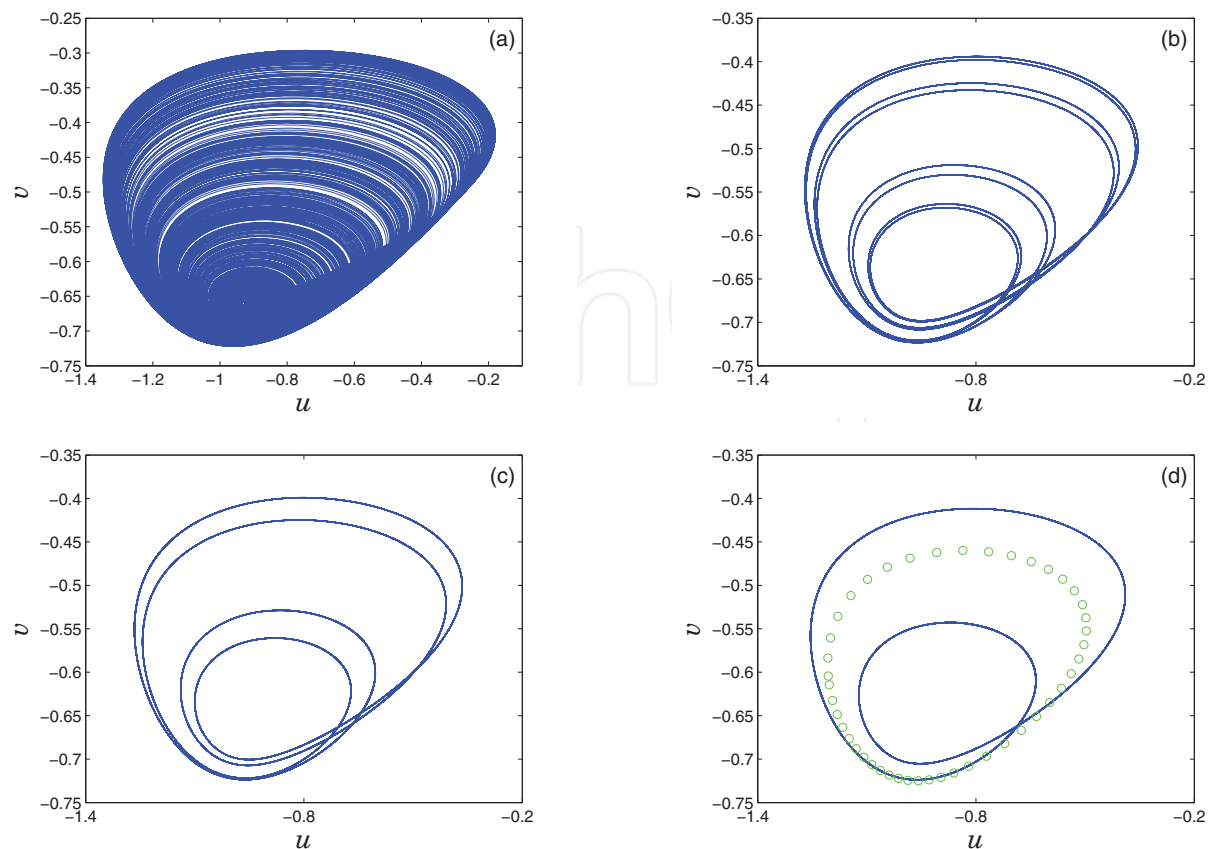where $\Theta(\vartheta) = 1$ if $\vartheta > 0$ and 0 otherwise; δ is the threshold parameter.

Fig. 14. State space of controlled system (33) at $a = 0.5$, $b = 0.b$, $\alpha = 0.1$, $c = 0.72$, $\iota = 0$, $\beta = 10$ and (a) $k = 0$; (b) $k = -0.0118$; (c) $k = -0.013$; (d) $k = -0.015$ (solid line) $k = -0.03$ (open circles).

5.2.1 Excitable regime

Looking for the travelling wave solution, obtain the following system of ODEs:

$$\ddot{u} + c\dot{u} + \mu\big(-u + \Theta(u - \delta) + v - \gamma\big) = 0$$

$$\dot{v} = \frac{1}{c}(\epsilon u - v) \tag{35}$$

where all derivatives are taken over the wave variable $\varrho = r - ct$.

System (35) demonstrates the "screw-type" chaos at some parameter values (Kahlert & Rössler, 1984). Applying the tanh-perturbation, the chaos is tamed to the periodic oscillations (Fig. 17).

5.2.2 Oscillatory regime

The adjustment of system's timescale and diffusion rate can stabilize the dynamics. Fig. 18(a) illustrates the emergence of low-frequency stabilizing modulation. Changing $k\beta$ leads to different patterns. Fig. 18(b) illustrates the temporal dynamics at the system middle point, i.e at $r = l/2$ where l is the system size.

6. Discussion and conclusions

The two control strategies are found to be effective: (i) altering a perturbation magnitude; (ii) reshaping a perturbation. In the majority of considered cases, the control represents
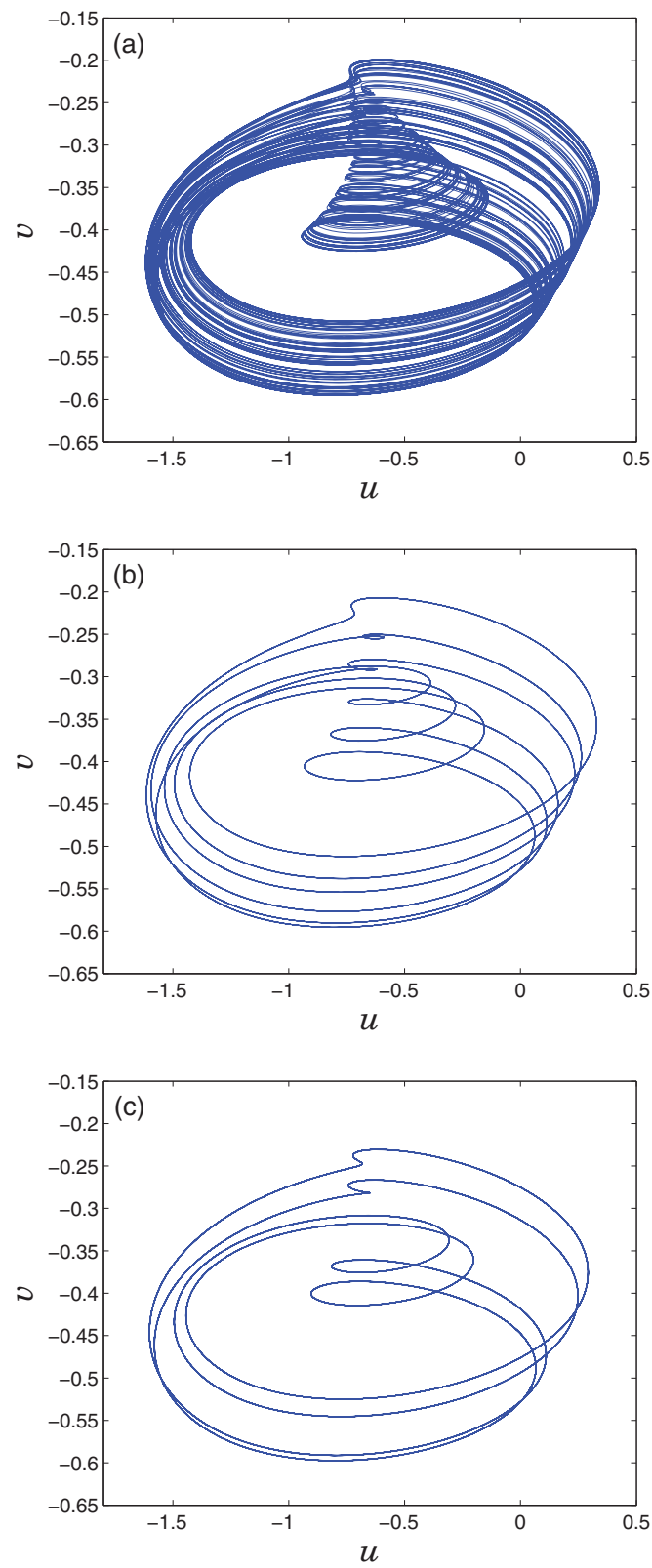
Fig. 15. State space of controlled system (33) at $a = 0.5$, $b = 0.5$, $\alpha = 0.1$, $c = 0.9$, $\rho = 0.55$, $\omega = 1$, $\beta = 100$ and (a) $k = 0$; (b) $k = -0.001$; (c) $k = -0.005$.
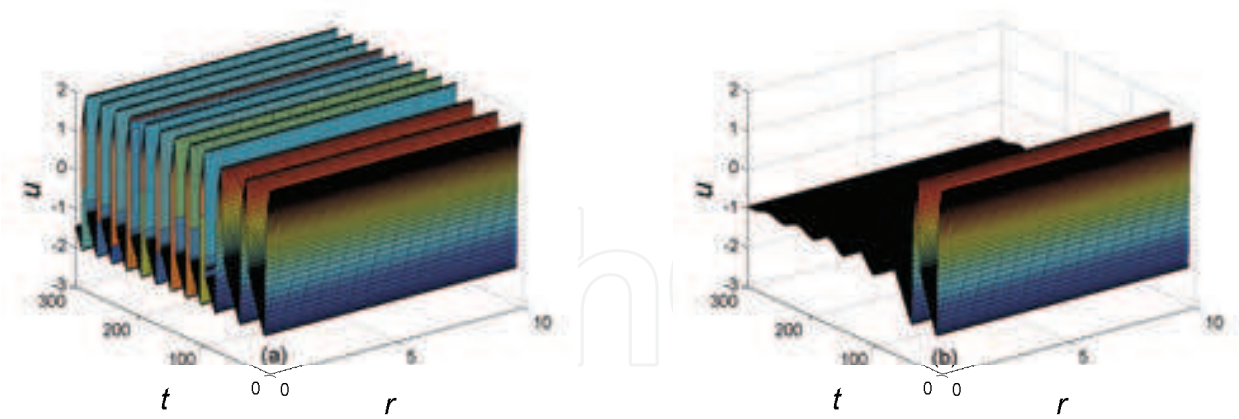
Fig. 16. Dynamics of controlled system (32) at $a = 0.5$, $b = 0.6$, $\alpha = 0.1$, $\delta = 0$ and (a) $k\beta = 0.99$; (b) $k\beta = -3.9$.
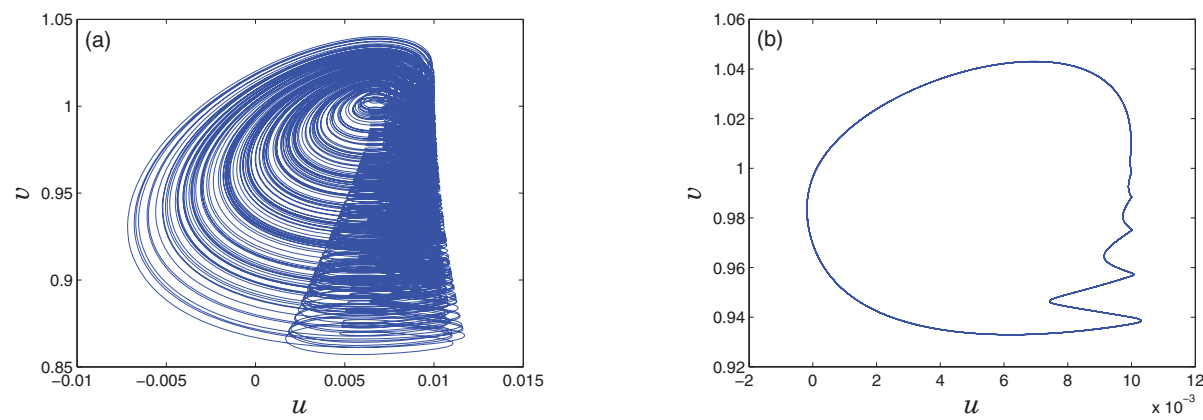

Fig. 17. State space of controlled system (35) at $\mu = 10$, $\gamma = 1$, $\delta = 0.01$, $\epsilon = 150$, $c = 3.5$, $\beta = 100$ and (a) $k = 0$; (b) $k = -0.21$.
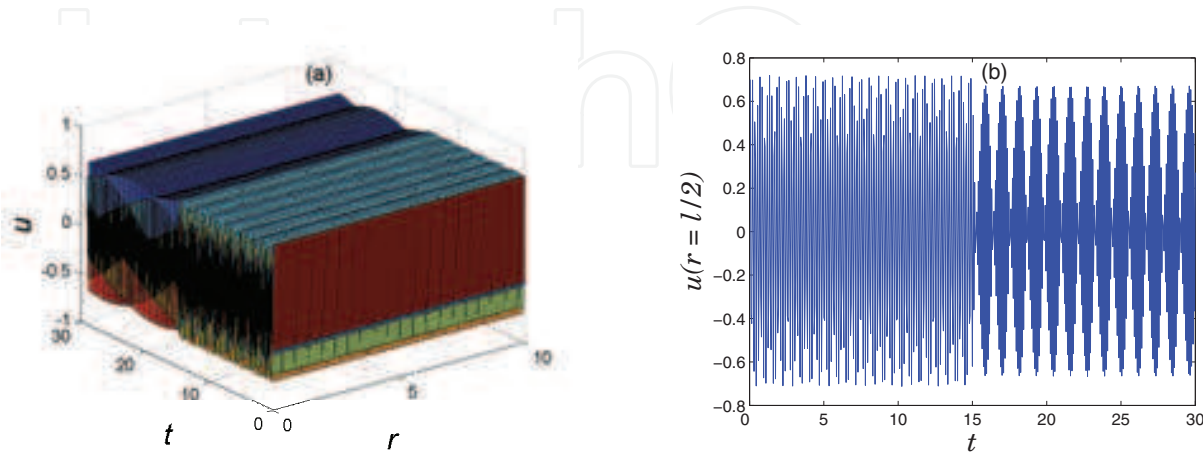
Fig. 18. Dynamics of controlled system (34) at $\mu = 10$, $\gamma = 1$, $\delta = 0.01$, $\epsilon = 150$ and (a) $k\beta = 0.5$; (b) $k\beta = 0.6$.

an addition of extra nonlinear damping to a system. Depending on the level of perturbation nonlinearity, two different scenarios take place. Recall that simple changing the tanh-perturbation slope transforms the feedback from near-linear to extremely nonlinear one. The above controls manifests themselves in (i) changing an oscillator natural damping; (ii) suppressing (enhancing) an external driving force, respectively. The perturbation shape, once again, reveals its significance determining the control mechanisms.

The occurrence of second scenario depends on the oscillator features. In our approach, a control perturbation is naturally locked to an oscillator velocity. If there is any phase shift between the velocity, and, hence, the control perturbation and the driving force, than a delayed version of control, i.e. $g(\dot{x}(t - \tau))$ with a time lag τ between the control perturbation and the driving force, will be most effective. Note, a phase of chaotic oscillator is determined using the approach developed in (Pikovsky et al., 1997; Rosenblum et al., 1996). When the phase difference between chaotic oscillations and a driving force exhibits large deviations, the coherence between the control action and the driving force can be destroyed. In this case independently on β, the control affects only an oscillator damping. This scenario is observed, for example, in the "broken egg" attractor (Ueda, 1992).

Though derived differently, in approximation $\dot{x} \approx \tau^{-1}(x(t) - x(t - \tau))$, the proposed control can be viewed as a continuous-delay control with saturation (or simply a continuous-delay control when $h(\dot{x}) = \dot{x}$) (Gauthier et al., 1994; Pyragas, 1992) adapted to the stabilization of fixed points. To control a fixed point, return time τ must tend to 0.

Recently our method was applied to mechanical systems where the forcing source has a limited available energy supply (de Souza et al, 2007). These oscillators, called non-ideal ones, are described by a combination of passive and active parts (the oscillator and the motor). The authors demonstrated the efficiency of approach applying the control altering the oscillation energy to the driving motor part.

Some of the existing methods of control can be reconsidered in the light of proposed approach. Look at so-called active control applied for suppressing oscillations driven by the dry friction forces (Heckl & Abrahams, 1996). These oscillations are produced by a mass-spring system sliding on a moving belt. The active control represents a feedback loop which senses the mass velocity, passes it to a filter, then to a phase shifter, to a variable-gain amplifier, and finally to shaker attached to the mass. The control force is $g(\dot{x}, \phi) = \alpha e^{i\phi}\dot{x}$ where α is a measure for amplification and ϕ is a phase shift. In terms of a time lag τ, $g(\dot{x}, \tau) = \alpha \dot{x}(t - \tau)$. Immediately, one find that at $\phi = 0$ ($\tau = 0$), or $\phi = \frac{\pi}{2}$ ($\tau = \frac{\pi}{2}$), the active control is nothing but the proposed energy alteration control. No surprise that, keeping positive α, the authors found their control to be optimal at $\phi = \frac{\pi}{2}$ ($\tau = \frac{\pi}{2}$). In this case, the averaged energy change brought about by the control decreases as $\langle \dot{x}(t)\dot{x}(t - \tau) \rangle = -\langle \dot{x}^2(t) \rangle$, which leads to recovering of lower energy repellors, and, generally, to the stabilization of dynamics.

The nonfeedback control methods can be reviewed in terms of energy alteration too. The resonance between a controlled signal and a control perturbation is usually the general condition for the efficient shift of the trajectory to a desired target, or, in other words, to altering the system energy. The phase of perturbation is used both to fine-tune the control or and to switch the drive direction on the opposite one, i.e. to switch between the directions of energy increase and decrease (Tereshko & Shchekinova, 1998).

An important issue is the application of control in practice. The authors in (Heckl & Abrahams, 1996) discussed the applications of their technique to real-life friction-driven oscillations, in particular, to a squeal noise. This disturbing type of noise occurs when there is a lateral progression of a wheel relative to a rail. The excited bending vibrations of the wheel

are radiated in the surrounding air and heard as intensive high pitched squeal. The authors present an experimental set where their control technique was tested.

A development of methods of controlling spatially-extended systems has great practical importance too. The considered excitable dynamics of active reaction-diffusion systems, for example, lies at the core of neuron functioning. Controlling the neural activity patterns can potentially treat mental, movement and sleep disorders, pain, and other illnesses associated with a neural system.

To summarize, we developed the control based on an alteration of oscillation energy. Since the approach utilizes a feedback that depends solely on the output signal, it is especially useful when the system parameters are inaccessible or hardly adjustable. The particular type of perturbation is rather relative — most important, it should comply with condition (5), which guarantees the monotonic change of a system oscillation energy. Then, the repellors are stabilized when the energy passes levels corresponding to their stable counterparts.

7. Acknowledgments

8. References

Alexeev, V.V. & Loskutov, A.Yu. (1987). Control of a system with a strange attractor through periodic parametric action. *Sov. Phys.-Dokl.* 32, 270–271.

Azevedo, A. & Rezende, S.M. (1991). Controlling chaos in spin-wave instabilities. *Phys. Rev. Lett.* 66, 1342–1345.

Baziliauskas, A.; Tamaševičius, A.; Bumeliene, S.; & Lindberg, E. (2001). Synchronization of chaotic Colpitts oscillators. *Scientic Proceedings of Riga Technical University, Ser. 7. Telecommunications and Electronics*, vol. 1, p. 55–58.

Braiman, Y. & Goldhirsch, I. (1991). Taming chaotic dynamics with weak periodic perturbations. *Phys. Rev. Lett.* 66, 2545–2548.

Cao, H. (2005). Primary resonant optimal control for homoclinic bifurcations in single-degree-of-freedom nonlinear oscillators. *Chaos, Solitons and Fractals* 24, 1387–1398.

Chacón, R. (1996). Geometrical resonance as a chaos eliminating mechanism. *Phys. Rev. Lett.* 77, 482–485.

Chacón, R. & Díaz Bejarano, J. (1993). Routes to suppressing chaos by weak periodic perturbations. *Phys. Rev. Lett.* 71, 3103–3106.

Chizhevsky, V.N. & Corbalán, R. (1996). Experimental observation of perturbation-induced intermittency in the dynamics of a loss-modulated CO_2 laser. *Phys. Rev. E* 54, 4576–4579.

Chizhevsky, V.N.; Corbalán, R. & Pisarchik, A.N. (1997). Attractor splitting induced by resonant perturbations. *Phys. Rev. E* 56, 1580–1584.

Chua, L.O.; Komuro, M. & Matsumoto, T. (1986). The double scroll family. *IEEE Trans. Circuits Syst.* CAS-33, 1072–1118.

Dangoisse, D.; Celet, J.-C. & Glorieux, P. (1997). Global investigation of the influence of the phase of subharmonic excitation of a driven system. *Phys. Rev. E* 56, 1396–1406.

De Feo, O.; Maggio, G.M. & Kennedy, M.P. (2000). The Colpitts oscillator: Families of periodic solutions and their bifurcations. *Int. J. Bifurcation and Chaos* 10, 935–958.

de Souza, S.L.T.; Caldas, I.L.; Viana, R.L.; Balthazar, J.M. & Brasil, R.M.L.R.F. (2007). A simple feedback control for a chaotic oscillator with limited power supply. *J. Sound and Vibration* 299, 664–671.

Ding, W.X.; She, H.Q.; Huang, W. & Yu, C.X. (1994). Controlling chaos in a discharge plasma. *Phys. Rev. Lett.* 72, 96–99.

FitzHugh, R. (1961). Impulses and physiological states in models of nerve membrane. *Biophys. J.* 1, 445–466.

Fronzoni, L.; Giocondo, M. & Pettini, M. (1991). Experimental evidence of suppression of chaos by resonant parametric perturbations. *Phys. Rev. A* 43, 6483–6487.

Garfinkel, A.; Spano, M.L.; Ditto, W.L. & Weiss, J. (1992). Controlling cardiac chaos. *Science* 257, 1230–1235.

Gauthier, D.J.; Sukow, D.W.; Concannon, H.M. & Socolar, J.E.S. (1994). Stabilizing unstable periodic orbits in a fast diode resonator using continuous time-delay auto-synchronization. *Phys. Rev. E* 50, 2343–2346.

Heckl, M.A. & Abrahams, I.D. (1996). Active control of friction-driven oscillations. *J. Sound and Vibrations* 193, 417–426.

Hikihara, T.; Touno, M.; & Kawagoshi, T. (1997). Experimental stabilization of unstable periodic orbit in magneto-elastic chaos by delayed feedback control. *Int. J. Bifurcation and Chaos* 7, 2837–2846.

Hodgkin, A. L. & Huxley, A. F. (1952). A quantitative description of membrane current and its application to conduction and excitation in nerve. *J. Physiol.* 117, 500–544.

Hunt, E.R. (1991). Stabilizing high-period orbits in a chaotic system: The diode resonator. *Phys. Rev. Lett.* 67, 1953–1955.

Hübinger, B.; Doerner, R; Martienssen, W.; Herdering, M.; Pitka, R. & Dressler, U. (1994). Controlling chaos experimentally in systems exhibiting large effective Lyapunov exponents. *Phys. Rev. E* 50, 932–948.

Hübler, A. & Lüscher, E. (1989). Resonant stimulation and control of nonlinear oscillators. *Naturwissenschaften* 76, 67–69.

Jackson, E.A. & Hübler, A. (1990). Periodic entrainment of chaotic logistic map dynamics. *Physica D* 44, 407–420.

Just, W.; Reckwerth, D.; Reibold, E. & Benner, H. (1999a). Influence of control loop latency on time-delayed feedback control. *Phys. Rev. E* 59, 2826–2829.

Just, W.; Reibold, D.E.; Benner, H.; Kacperski, K.; Fronczak, P. & Hołyst, J. (1999b). Limits of time-delayed feedback control. *Phys. Lett. A* 254, 158–164.

Kahlert, C. & Rössler, O. E. (1984). Chaos as a limit in a boundary value problem. *Z. Naturforsch.* 39a, 1200–1203.

Kennedy, M.P. (1994). Chaos in the Colpitts oscillator. *IEEE Trans. Circuits Syst.* 41, 771–774.

Kivshar, Y.S.; Rödelsperger, F. & Benner, H. (1994). Suppression of chaos by nonresonant parametric perturbations. *Phys. Rev. E* 49, 319–324.

Kolosov, G.E. (1999). *Optimal Design of Control Systems: Stochastic and Deterministic Problems*, Marcel Dekker, Inc., New York.

Landau, L.D. & Lifshitz, E.M. (1976). *Mechanics (Course of Theoretical Physics, Vol. 1)*, Pergamon Press, Oxford, third edition.

Lima, R. & Pettini, M. (1990). Suppression of chaos by resonant parametric perturbations. *Phys. Rev. A* 41, 726–733.

Liu, Y. & Leite, J.R. (1994). Control of Lorenz chaos. *Phys. Lett. A* 185, 35–37.

Meucci, R. Gadomski, W.; Ciofini, M. & Arecchi, F.T. (1994). Experimental control of chaos by means of weak parametric perturbations. *Phys. Rev. E* 49, R2528–R2531.

Myneni, K; Barr, Th. A.; Corron, N.J. & Pethel, S.D. (1999). New method for the control of fast chaotic oscillations. *Phys. Rev. Lett.* 83, 2175–2178.

Ott, E.; Grebogi, C. & Yorke, J.A. (1990). Controlling chaos. *Phys. Rev. Lett* 64, 1196-1199.

Peng, B., Petrov, V. & Showalter, K. (1991). Controlling Chemical Chaos. *J. Phys. Chem.* 95, 4957–4959.

Pikovsky, A.S.; Rosenblum, M.G.; Osipov, G.V. & Kurths, J. (1997). Phase synchronization of chaotic oscillators by external driving. *Physica D* 104, 219–238.

Pyragas, K. (1992). Continuous control of chaos by self-controlling feedback. *Phys. Lett. A* 170, 421–428.

Pyragas, K. (1995). Control of chaos via extended delay feedback. *Phys. Lett. A* 206, 323–330.

Qu, Z.; Hu, G.; Yang, G. & Qin, G. (1995). Phase effect in taming nonautonomous chaos by weak harmonic perturbations. *Phys. Rev. Lett.* 74, 1736–1739.

Rajesekar, S. & Lakshmanan, M. (1994). Bifurcation, chaos and suppression of chaos in FitzHughŰNagumo nerve conduction modelation. *J. Theor. Biol.* 166, 275–288.

Ramesh, M. & Narayanan, S. (1999). Chaos control by nonfeed- back methods in the presence of noise. *Chaos, Solitons and Fractals* 10, 1473–1489.

Reyl, C.; Flepp, L.; Badii, R. & Brun, E. (1993). Control of NMR-laser chaos in high-dimensional embedding space. *Phys. Rev. E* 47, 267–272.

Rinzel, J. & Keller, J.B. (1973). Traveling wave solutions of a nerve conduction equation. *Biophys. J.* 13, 1313-1337.

Rosenblum, M.G.; Pikovsky, A.S. & Kurths, J. (1996). Phase synchronization of chaotic oscillators. *Phys. Rev. Lett.* 76, 1804–1807.

Rödelsperger, F., Kivshar, Y.S. & Benner, H. (1995). Reshaping-induced chaos suppression. *Phys. Rev. E* 51, 869-872.

Scott, A. F. (1975). The electrophysics of a nerve fiber. *Rev. Mod. Phys.* 47, 487–533.

Shinbrot, T.; Ott, E.; Grebogi, C. & Yorke, J.A. (1993). Using small perturbations to control chaos. *Nature* 363, 411–417.

Simmendinger, C.; Hess, O. & Wunderlin, A. (1998). Analytical treatment of delayed feedback control. *Phys. Lett. A* 245, 253–258.

Socolar, J.E.S.; Sukow, D.W.; & Gauthier, D.J. (1994). Stabilizing unstable periodic orbits in fast dynamical systems. *Phys. Rev. E* 50, 3245–3248.

Tereshko, V. (2009). Control and identification of chaotic systems by altering their energy. *Chaos, Solitons and Fractals* 40, 2430Ű-2446.

Tereshko, V.; Chacón, R. & Carballar, J. (2004a). Controlling the chaotic Colpitts oscillator by altering its oscillation energy. *Proc. 12th Intern. IEEE Workshop on Nonlinear Dynamics of Electronic Systems (NDES 2004)*, Évora, Portugal, p. 336.

Tereshko, V.; Chacón, R. & Preciado, V. (2004b). Controlling chaotic oscillators by altering their energy. *Phys. Lett. A* 320, 408–416.

Tereshko, V. & Shchekinova, E. (1998). Resonant control of the Rossler system. *Phys. Rev. E* 58, 423–426.

Ueda, Y. (1992). *The Road to Chaos*, Aerial Press, Santa Cruz.

Wu, S. (1987). Chua's circuit family. *Proc. IEEE* 75, 1022–1032.
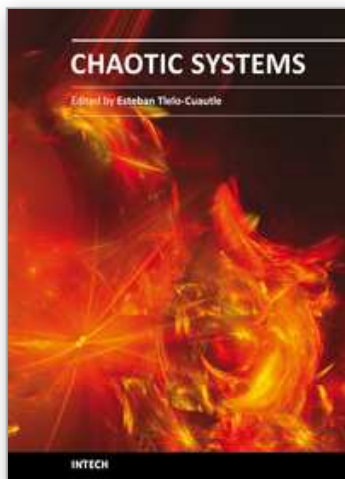
Chaotic Systems

Edited by Prof. Esteban Tlelo-Cuautle

ISBN 978-953-307-564-8

Hard cover, 310 pages

Publisher InTech

Published online 14, February, 2011

Published in print edition February, 2011

This book presents a collection of major developments in chaos systems covering aspects on chaotic behavioral modeling and simulation, control and synchronization of chaos systems, and applications like secure communications. It is a good source to acquire recent knowledge and ideas for future research on chaos systems and to develop experiments applied to real life problems. That way, this book is very interesting for students, academia and industry since the collected chapters provide a rich cocktail while balancing theory and applications.

INTECH

open science | open minds